molecules become quite resistant to rapid fluorine attack.

A comparison of the control NPF/N-6 with PF/N-6 (Figure 3) indicates that although general upward movement in the product distribution toward higher fluorination occurs, "anomalous" production of *F*-neopentane also occurs. This "anomalous" production of *F*-neopentane in reactions PF/N-4–6 must be due to a "hot molecule" effect. That is, fluorinated neopentanes attacked by atomic fluorine in the photochemical stage become chemically excited and thus more reactive toward fluorine. These "hot molecules" react much more rapidly than nonexcited fluoroneopentanes.

The results seen in reaction PF/N-7 result from two main factors. Molecules are more highly fluorinated when they enter the photochemical stage (cf. F/N-20 (Figure 2) vs. PF/N-7 (Figure 3)), and the fluorine concentration is high enough to exceed the threshold for radical chain propagation throughout the reaction mixture. Both factors contribute toward perfluorination while molecular integrity is maintained to a high degree.

The fluorination of 1,4-dioxane dramatizes the effectiveness of the photochemical stage (Figure 4). The crude product collected from the reactor is better than 90% pure *F*-1,4-dioxane in yields approaching 60%. The extremely difficult direct fluorination of cyclohexane to perfluorocyclohexane can be accomplished in yields exceeding 30% and a product purity in excess of 90% direct from the reactor. The low yields are due to tar formation in stage one which we should be able to eliminate by reducing the fluorine concentration gradient at this stage.

### Absence of Hydrogen Fluoride Solvolysis

The direct fluorination reaction produces a molecule of hydrogen fluoride for every hydrogen substituted. It was of interest to determine whether acid-catalyzed cleavage would occur in the reactor system to an appreciable extent. The very acid sensitive ketal, 2,2-dimethyl-1,3-dioxolane, was chosen for this determination. The results indicate that HF solvolysis of such groupings is not a problem. It was possible to produce fluoro analogues of the 1,3-dioxolane in very good yields with almost no evidence of HF solvolysis (Figure 5). The photochemical perfluorination went uneventfully and actually produced higher overall yields than the 1,4-dioxane. Whether this lack of solvolysis is general will, of course, requires reaction of many different compounds possessing different functionalities.

### Summary

The multistaged aerosol fluorination reactor achieves near optimum control over the potentially violent direct fluorination reaction. This system meets all of the criteria enumerated earlier which we, by experience, believe contribute to high yield direct fluorination reactions. It additionally has other distinct advantages in that the degree of fluorination may be controlled: it is a flow process, the process is not highly dependent on the physical properties of the reactant to be fluorinated, reactant throughputs may be varied over a considerable range for a given design, fluorine concentration and temperature conditions may be taylored to the reactivity of the reactant, and most importantly the observation of nonstatistical substitution effects suggests that this system might permit the elusive achievement of selectivity in direct fluorinations.

**Acknowledgment.** This work was supported in part by the Office of Naval Research whose support is gratefully acknowledged. We also wish to thank the Research Corp., Cottrell Research Fund for a starter grant (to J.L.A.), and the South Carolina NMR Facility and Dr. Michelle Buchanan (ORNL) for $^{19}F$ NMR.

**Supplementary Material Available:** Table A, IR, mass spectra, and elemental analyses for partially fluorinated neopentanes (7 pages). Ordering information is given on any current masthead page.

# Crystal and Molecular Structure of [Tris(4,5-diisopropylimidazol-2-yl)phosphine]dichlorozinc(II)–Bis[*N*,*N*-dimethylformamide]

**Randy J. Read and Michael N. G. James***

*Contribution from the MRC Group in Protein Structure and Function, Department of Biochemistry, University of Alberta, Edmonton, Alberta, Canada, T6G 2H7.*
*Received February 3, 1981. Revised Manuscript Received June 29, 1981*

**Abstract:** The crystal structure of [tris(4,5-diisopropylimidazol-2-yl)phosphine]dichlorozinc(II), which crystallized with two molecules of *N*,*N*-dimethylformamide per molecule, has been determined by X-ray methods and refined to a final agreement factor $R = 0.037$ for the 2361 reflections having $I > 3\sigma(I)$. The compound crystallizes in space group *Pnma* with $a = 10.323$ (5) Å, $b = 18.648$ (9) Å, $c = 22.220$ (15) Å, and $Z = 4$. Zn(II) is tetrahedrally coordinated by the N atoms of the three substituted imidazole rings and one of the chloride ions. The molecule has one mirror plane of symmetry which is coincident with the space group symmetry. The title compound is a structural analogue of that part of the active site of the enzyme carbonic anhydrase which consists of Zn(II), three histidine ligands, and a water molecule.

Carbonic anhydrase is a zinc-containing enzyme which catalyzes the reaction

$$CO_2 + H_2O \rightleftharpoons H^+ + HCO_3^-$$

The crystal structures of the isoenzymes from human erythrocytes, human carbonic anhydrases B (HCAB)[1] and C (HCAC)[2], have been determined to 2.2- and 2.0-Å resolution, respectively. These structures show that, in the active site, three histidine residues are coordinated through imidazole N atoms to Zn(II) in an approximately tetrahedral configuration. The fourth ligand is probably a water molecule or hydroxyl ion. [Tris(4,5-diiso-

(1) Kannan, K. K.; Notstrand, B.; Fridborg, K.; Lövgren, S.; Ohlsson, A.; Petef, M. *Proc. Natl. Acad. Sci. U.S.A.* **1975**, *72*, 51–55.

(2) Liljas, A.; Kannan, K. K.; Bergstēn, P.-C.; Waara, I.; Fridborg, K.; Strandberg, B.; Carlbom, U., Järup, L.; Lövgren, S.; Petef, M. *Nature (London), New Biol.* **1972**, *235*, 1–7.

0002-7863/81/1503-6947$01.25/0 

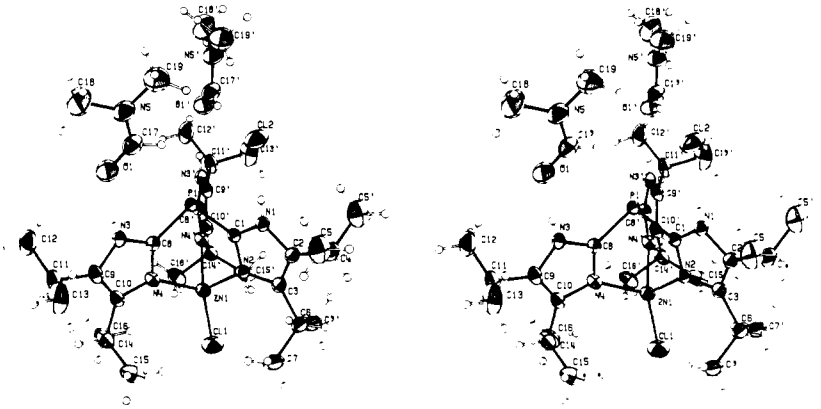

**Figure 1.** Stereoscopic view of the crystal structure, showing the asymmetric unit and its mirror image. Thermal ellipsoids are drawn at 35% probability for nonhydrogen atoms, and hydrogen atoms are represented by spheres of arbitrary radius.

propylimidazol-2-yl)phosphine]dichlorozinc(II) was synthesized in an attempt to mimic the Zn(II) coordination sphere and catalytic activity of carbonic anhydrase.[3]

## Experimental Section

**[Tris(4,5-diisopropylimidazol-2-yl)phosphine]dichlorozinc(II).** Stoichiometric quantities of the ligand and $ZnCl_2$ were mixed and dissolved in a minimum volume of ethanol (95%). A portion of the ethanol solution was then mixed in an approximate 1:4 ratio with *N,N*-dimethylformamide (DMF) and the complex crystallized from this solution by controlled evaporation. The crystal density, measured by flotation in an aqueous CsCl solution, and subsequent structure solution confirmed that each ligand molecule is accompanied by two DMF molecules of crystallization.

**Crystal Data:** $C_{27}H_{45}N_6P\cdot ZnCl_2\cdot 2C_3H_7NO$, $M_r$ = 767.1, orthorhombic, *Pnma*, $a$ = 10.323 (5) Å, $b$ = 18.648 (9) Å, $c$ = 22.220 (15) Å, $V$ = 4277 (7) Å$^3$, $d_{measd}$ = 1.20 (1) g cm$^{-3}$, $d_{calcd}$ = 1.191 g cm$^{-3}$, $Z$ = 4, $F(000)$ = 1632, Cu K$\alpha$ radiation, $\lambda$ = 1.5418 Å, $\mu$(Cu K$\alpha$) = 26.2 cm$^{-1}$.

**Structure Solution and Refinement.** Preliminary oscillation, Weissenberg, and precession photographs showed that the crystals had *mmm* diffraction symmetry and that the diffraction pattern exhibited systematic absences $hk0$, $h = 2n + 1$, and $0kl$, $k + l = 2n + 1$, consistent with space groups $Pn2_1a$ and *Pnma*. Intensity data were collected from a single crystal (0.4 × 0.4 × 0.2 mm) with a Picker FACS-1 diffractometer by using Ni-filtered Cu K$\alpha$ radiation. The unit-cell parameters were determined by least-squares refinement of the positions of 15 accurately centered reflections ($2\theta > 65°$). Crystal decay was monitored and corrected with five control reflections; their intensities decreased linearly to an average final value that was 19.5% less than their average initial value. A total of 5740 reflections in the range $0° < 2\theta < 110°$ was measured in the $\theta/2\theta$ scan mode, and equivalent reflections ($hkl$, $hk\bar{l}$) were averaged ($R_{merge}$ = 2.11%) to obtain 3067 unique reflections of which 2361 had $I > 3\sigma(I)$. The measured intensities were corrected for absorption by the empirical method of North, Phillips, and Mathews[4] (maximum absorption correction factor equals 1.206).[5]

The position of the Zn atom was determined from a sharpened Patterson synthesis in which the origin peak had been removed (the origin of the $y$ axis is arbitrary for $Pn2_1a$ but, on the basis of the unit-cell content, $Z$ = 4, the Zn is constrained to lie on the mirror at $y = {}^1/_4$ in *Pnma*), and Fourier maps were calculated for the two alternative space groups. The map for $Pn2_1a$ was uninterpretable, while the map for *Pnma* showed clearly the positions of the Zn, P, and Cl atoms.[6] This choice

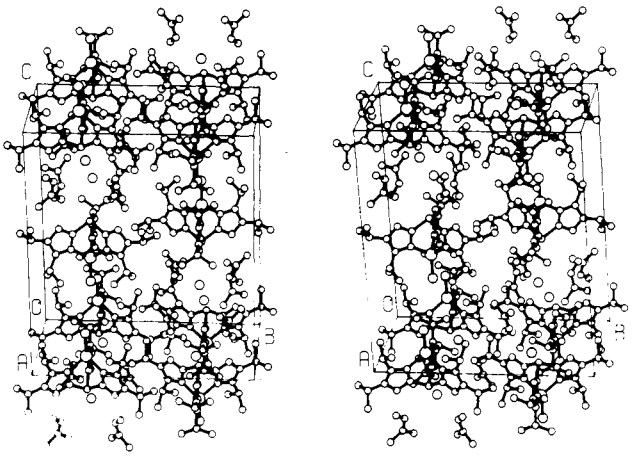

**Figure 2.** Stereoscopic view of the contents of the unit cell.

of the centric alternative is also indicated by statistics on the distribution of $|E|$ values. The remaining nonhydrogen atoms, including those of the solvent molecule, were located in subsequent difference Fourier maps. When positional and anisotropic thermal parameters for these atoms were refined by full-matrix least-squares refinement, 30 of the 31 H atoms in the asymmetric unit were found from subsequent difference maps. The remaining H(183) was placed in its expected tetrahedral position bonded to C(18) (see Figure 1). Positional and thermal parameters (anisotropic for nonhydrogen, isotropic for hydrogen atoms) were refined for all atoms. A comparison of calculated and observed $|F|$'s indicated that four reflections (020, 060, 080, and 002) were affected by secondary extinction; these were removed from further cycles of refinement. The refinement converged at a residual ($R = \sum||F_o| - k|F_c||/\sum|F_o|$) of 0.037 and a weighted residual ($R_w = [\sum w||F_o| - k|F_c||^2/\sum w|F_o|^2]^{1/2}$, where $w = 1/(\sigma(F))^2$) of 0.056. In a final difference map, there were several significant features. The largest positive peak, which we have interpreted as Zn–Cl(1) bonding density, had a height of 0.30 e Å$^{-3}$. Positive difference density was also associated with the bonds C(1)–N(2) (peak height of 0.23 e Å$^{-3}$), Zn–N(4) (0.16 e Å$^{-3}$), and C(8)–N(4) (0.15 e Å$^{-3}$). Another positive peak, which had a height of 0.18 e Å$^{-3}$, was near Cl(2). The only other difference electron density above 0.15 e Å$^{-3}$ was an approximately spherical feature centered on a point about 1.14 Å from the phosphorus, with a peak height of 0.27 e Å$^{-3}$, which we have interpreted as lone-pair electron density. The largest negative peak, which was centered on the Zn atom, had a peak height of −0.56 e Å$^{-3}$. The next largest negative features were centered on the other heavy atoms, i.e., Cl(2) (peak height of −0.29 e Å$^{-3}$), P (−0.28 e Å$^{-3}$), and Cl(1) (−0.27 e Å$^{-3}$). Other significant features of negative density, which had peak

(3) Brown, R. S.; Curtis, N. J.; Huguet, J. *J. Am. Chem. Soc.*, following paper in this issue.

(4) North, A. C. T.; Phillips, D. C.; Mathews, F. S. *Acta Crystallogr., Sect. A* **1968**, *A24*, 351–359.

(5) Corrections for Lorentz and polarization effects and all structure solution and refinement calculations were performed with the programs of the XRAY 70 system. (Stewart , J. M.; Kundell, F. A.; Baldwin, J. C. "The XRAY 70 System"; Computer Science Center: University of Maryland, College Park, MD, 1970.) Atomic scattering factors of the nonhydrogen atoms were those found in: Cromer, D. T.; Mann, J. B. *Acta Crystallogr., Sect. A* **1968**, *A24*, 321–324; anomalous dispersion corrections were obtained from: "International Tables for X-ray Crystallography"; Kynoch Press: Birmingham, England, 1974; Vol. IV, pp 149–150. Hydrogen atom scattering factors are from: Mason, R.; Robertson, G. B. "Advances in Structure Research by Diffraction Methods"; Brill, R., Mason, R. Eds.; Interscience: New York, 1966; Vol. 2, p 57.

(6) C. G. Broughton's map display and molecule manipulation program M3, which runs on an MMS-X interactive graphics system (Barry, C. D.; Molnar, C. E.; Rosenberger, F. U. "Technical Memorandum No. 229"; Computer Systems Laboratory: Washington University, St. Louis, Mo, 1976), was invaluable in electron density interpretation, assignment of initial atomic coordinates and model-building experiments. As well, it was used to draw Figure 5. C. K. Johnson's ORTEP was used for Figure 1, and W. D. S. Motherwell's PLUTO was used for Figures 2 and 4.

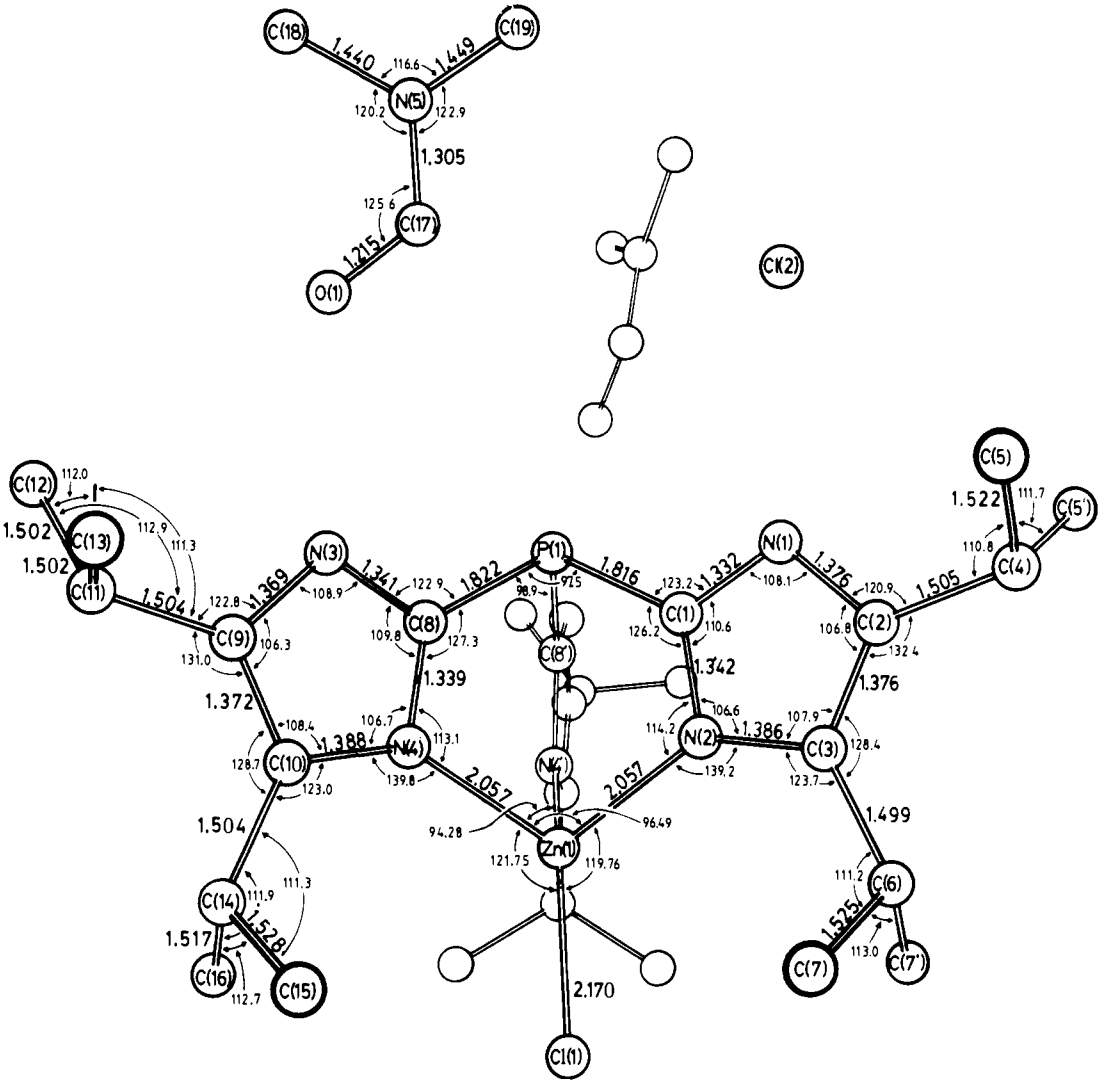


**Figure 3.** Perspective view showing unique bond lengths and angles involving nonhydrogen atoms. Standard deviations of bond lengths are of the order of 0.002 Å for bonds involving Zn and P and 0.004 Å for other bonds. Standard deviations of bond angles are of the order of 0.1° for angles involving Zn and P and 0.2° for other bond angles.

heights ranging from −0.14 to −0.24 e $Å^{-3}$, were found inside and outside the imidazole rings and at the center of the ligand molecule (i.e., between P and Zn). Peaks corresponding to all hydrogen atoms could be seen in a difference map calculated with the nonhydrogen atoms of the final refined model. However, the electron density for H(183), which had an isotropic B factor of 25 (5) $Å^2$, was poorly resolved from that of H(182). Final positional and thermal parameters for all atoms are listed in Table I.[7]

## Results and Discussion

The Zn–ligand complex has approximate *3m* symmetry (see Figure 1), with only one of the possible molecular mirror planes used in the crystal packing (see Figure 2). The Zn, P, and two Cl atoms and one of the imidazole rings lie on the crystallographic mirror plane; the other two imidazole rings and the solvent DMF molecules are mirror related. An examination of Figure 3 shows that, with few exceptions, bond lengths and angles involving corresponding atoms are not significantly different.

The Zn(II) atom has approximate tetrahedral coordination to one chloride ion and three N atoms. To the best of our knowledge, this is the first crystal structure in which Zn(II) has three N ligands and an anionic ligand. Comparisons were made with structures in which a tetrahedral Zn(II) has either two or four N ligands. The Zn–N bond lengths (both 2.057 (2) Å) do not differ significantly from those of [bis(4,5-diisopropyl-1-methyl-2-imidazolyl) ketone]dibromozinc(II)[8] (2.041 (9) and 2.053 (10) Å) but are longer than those of tetrakis(imidazole)zinc(II) perchlorate[9] (two crystallographically independent distances of 1.997 (7) and 2.001 (7) Å). The Zn–Cl bond length (2.170 (2) Å) is within the range seen in ammonium tetrachlorozincate(II)[10] (mean 2.250 Å, range 2.11–2.404 Å). Angles about the Zn atom deviate significantly from tetrahedral angles; the Cl–Zn–N angles are larger (119.76 (7) and 121.75 (5)°) and the N–Zn–N angles are smaller (96.49 (7) and 94.28 (7)°).

The P–C bond lengths and angles were compared with those of other aromatic phosphines. The P–C bonds are slightly shorter (1.816 (3) and 1.822 (2) Å) than those seen either in tri-*o*-tolylphosphine[11] (mean 1.835 Å, range 1.830–1.837 Å) or in tri-*m*-tolylphosphine[12] (mean 1.835 Å, range 1.829–1.838 Å). The C–P–C bond angles are significantly smaller (97.5 (1) and 98.9 (1)°) than those in tri-*o*-tolylphosphine (mean 102.6°, range 101.6–103.4°) or tri-*m*-tolylphosphine (mean 101.7°, range 100.6–102.2°).

(7) See the paragraph regarding supplementary material at the end of this article.

(8) Read, R. J.; James, M. N. G. *Acta Crystallogr., Sect. B* **1980**, *B36*, 3100–3102.
(9) Bear, C. A.; Duggan, K. A.; Freeman, H. C. *Acta Crystallogr., Sect. B* **1975**, *B31*, 2713–2715.
(10) Mikhail, I. *Acta Crystallogr., Sect. B* **1980**, *B36*, 2126–2128.
(11) Cameron, T. S.; Dahlèn, B. *J. Chem. Soc., Perkin Trans. 2* **1975**, 1737–1751.
(12) Cameron, T. S.; Howlett, K. D.; Miller, K. *Acta Crystallogr., Sect. B* **1978**, *B34*, 1639–1644.

Table I. Fractional Atomic Coordinates (×10⁴) and Thermal Parameters (Å²) (esd's in parentheses)[a]

| atom | x/a | y/b | z/c | $B_{equiv}$ |
|---|---|---|---|---|
| Zn(1) | 5569.7 (4) | 2500 | 3994.6 (2) | 2.96 (1) |
| Cl(1) | 5663 (1) | 2500 | 3018.8 (4) | 5.53 (3) |
| Cl(2) | 2301 (1) | 2500 | 6612.9 (4) | 6.75 (4) |
| P(1) | 5339.8 (6) | 2500 | 5468.1 (3) | 2.44 (2) |
| C(1) | 3867 (3) | 2500 | 5021 (1) | 2.42 (7) |
| C(2) | 1797 (3) | 2500 | 4800 (1) | 2.92 (7) |
| C(3) | 2492 (3) | 2500 | 4272 (1) | 2.99 (7) |
| C(4) | 366 (3) | 2500 | 4928 (2) | 3.83 (9) |
| C(5) | −29 (4) | 3175 (2) | 5266 (2) | 6.06 (11) |
| C(6) | 1991 (4) | 2500 | 3639 (1) | 3.72 (9) |
| C(7) | 2385 (4) | 3182 (2) | 3307 (1) | 4.90 (9) |
| C(8) | 6146 (2) | 3242 (1) | 5089 (1) | 2.65 (5) |
| C(9) | 7109 (2) | 4289 (1) | 4972 (1) | 3.40 (5) |
| C(10) | 6997 (2) | 3964 (1) | 4420 (1) | 3.31 (5) |
| C(11) | 7661 (3) | 5006 (1) | 5148 (1) | 4.42 (7) |
| C(12) | 8453 (4) | 4974 (2) | 5714 (2) | 6.32 (11) |
| C(13) | 6622 (4) | 5569 (2) | 5181 (3) | 7.81 (16) |
| C(14) | 7461 (3) | 4227 (1) | 3818 (1) | 4.58 (7) |
| C(15) | 6325 (4) | 4414 (2) | 3406 (2) | 6.36 (10) |
| C(16) | 8405 (4) | 3707 (2) | 3529 (2) | 5.66 (10) |
| C(17) | 5294 (3) | 3740 (2) | 6898 (1) | 5.11 (8) |
| C(18) | 5935 (8) | 4390 (4) | 7772 (2) | 10.37 (20) |
| C(19) | 4170 (5) | 3508 (3) | 7834 (2) | 8.58 (15) |
| N(1) | 2685 (2) | 2500 | 5262 (1) | 2.65 (6) |
| N(2) | 3798 (2) | 2500 | 4418 (1) | 2.63 (6) |
| N(3) | 6571 (2) | 3826 (1) | 5380 (1) | 2.82 (5) |
| N(4) | 6381 (2) | 3308 (1) | 4499 (1) | 2.96 (4) |
| N(5) | 5107 (2) | 3886 (1) | 7466 (1) | 5.59 (6) |
| O(1) | 6097 (2) | 4022 (1) | 6576 (1) | 6.30 (6) |
| atom | x/a | y/b | z/c | $B_{iso}$ |
| H(11) | 2566 (33) | 2500 | 5634 (17) | 3.6 (7) |
| H(31) | 6522 (18) | 3873 (10) | 5719 (10) | 1.1 (4) |
| H(41) | −54 (34) | 2500 | 4541 (16) | 3.5 (6) |
| H(51) | −1038 (54) | 3150 (24) | 5314 (18) | 9.0 (1.1) |
| H(52) | 363 (33) | 3138 (17) | 5663 (16) | 5.5 (7) |
| H(53) | 129 (45) | 3606 (27) | 5034 (20) | 8.2 (1.0) |
| H(61) | 1056 (38) | 2500 | 3650 (12) | 2.7 (6) |
| H(71) | 1974 (36) | 3629 (20) | 3587 (15) | 6.9 (8) |
| H(72) | 3328 (40) | 3225 (18) | 3263 (15) | 6.1 (8) |
| H(73) | 2162 (37) | 3188 (19) | 2936 (19) | 6.9 (8) |
| H(111) | 8172 (47) | 5147 (25) | 4870 (19) | 8.7 (1.1) |
| H(121) | 7952 (51) | 4833 (26) | 6028 (19) | 8.5 (1.2) |
| H(122) | 8853 (34) | 5444 (20) | 5780 (14) | 5.9 (6) |
| H(123) | 9010 (44) | 4606 (26) | 5714 (19) | 7.9 (1.0) |
| H(131) | 6834 (40) | 6037 (28) | 5279 (17) | 7.9 (9) |
| H(132) | 6078 (47) | 5415 (23) | 5501 (19) | 7.5 (1.1) |
| H(133) | 6327 (60) | 5649 (27) | 4744 (24) | 10.0 (1.3) |
| H(141) | 7974 (31) | 4633 (17) | 3895 (12) | 4.9 (6) |
| H(151) | 5907 (37) | 4792 (20) | 3611 (15) | 5.9 (8) |
| H(152) | 5656 (55) | 4015 (34) | 3311 (26) | 10.5 (1.4) |
| H(153) | 6567 (42) | 4588 (23) | 3013 (18) | 8.0 (9) |
| H(161) | 8661 (43) | 3889 (22) | 3202 (20) | 7.7 (9) |
| H(162) | 7974 (39) | 3237 (22) | 3454 (15) | 6.7 (8) |
| H(163) | 9183 (44) | 3640 (21) | 3782 (21) | 7.4 (9) |
| H(171) | 4706 (30) | 3397 (17) | 6783 (13) | 4.3 (6) |
| H(181) | 6334 (68) | 4716 (31) | 7424 (29) | 12.8 (1.6) |
| H(182) | 5416 (69) | 4599 (39) | 8026 (33) | 12.5 (2.0) |
| H(183) | 6601 (145) | 4192 (72) | 7970 (64) | 24.7 (5.3) |
| H(191) | 3616 (63) | 3204 (30) | 7578 (26) | 11.4 (1.4) |
| H(192) | 3563 (59) | 3943 (32) | 8047 (24) | 11.1 (1.4) |
| H(193) | 4664 (49) | 3304 (28) | 8190 (25) | 9.4 (1.2) |

[a] Isotropic thermal parameters were used for H atoms. For all other atoms, equivalent isotropic temperature factors ($B_{eq} = {}^4/_3(\beta_{11}a^2 + \beta_{22}b^2 + \beta_{33}c^2)$) are given.

Table II. Least-Squares Planes Calculations[b]

Plane 1:[a] $Y = 0.25$

Plane 2: $9.183X - 8.174Y + 2.856Z = 4.444$

$\sigma = 0.003$ Å

| | d | | d |
|---|---|---|---|
| Zn(1) | −0.232 | C(14) | 0.042 |
| Cl(1) | −0.425 | N(3)* | −0.001 |
| P(1) | −0.023 | N(4)* | −0.004 |
| C(8)* | 0.003 | O(1) | −0.255 |
| C(9)* | −0.002 | H(31) | 0.01 |
| C(10)* | 0.004 | H(111) | 0.24 |
| C(11) | −0.031 | H(141) | 0.20 |

Plane 3: $-6.810X + 13.366Y - 5.023Z = -2.070$

$\sigma = 0.021$ Å

| | d | | d |
|---|---|---|---|
| C(17)* | −0.001 | N(5)* | 0.035 |
| C(18)* | −0.009 | O(1)* | −0.009 |
| C(19)* | −0.017 | H(31) | −0.07 |
| N(3) | 0.006 | H(171) | 0.00 |

Interplane Dihedral Angles

| planes | dihedral angle, deg |
|---|---|
| plane 1–plane 2 | 64.0 |
| plane 1–plane 3 | 44.2 |
| plane 2–plane 3 | 21.6 |

[a] This is the crystallographic mirror plane. [b] The equations of the planes are expressed in direct space as $pX + qY + rZ = s$. $d$ is the perpendicular distance (Å) from the plane. Atoms marked with an asterisk were included in the least-squares plane calculation.

Although the crystal structure of the free ligand is not known, it is likely that the C–P–C bond angles are similar to those of the tolylphosphines, since the hybridization of the C atoms is the same and the size of an imidazole ring is similar to that of toluene. The tridentate coordination to Zn(II) must therefore induce a strain on the ligand. If the Zn atom were to move closer to the P atom, the C–P–C bond angles could open toward the values found in less constrained systems while maintaining the same N–Zn bond distance (assuming that the P(1)–C(1)–N(2) and P(1)–C(8)–N(4) bond angles are the least flexible). At the same time, angles about Zn would become closer to tetrahedral. There are two influences which probably act to prevent this. In the first place, Zn and P are already in fairly close contact (3.283 (2) Å). The second influence is the large change in bond angles about the ligand N atoms that would be required by this conformational change. One might assume that the most favorable configuration for the N–Zn bond would be one in which the bisector of the C–N–C bond angle is coincident with the N–Zn vector. Indeed, such an assumption is supported by the structure of tetrakis(imidazole)zinc(II) perchlorate[9] in which the angles between the C–N–C bisector and the N–Zn vector are 1.4 and 5.5° for the two crystallographically independent imidazole rings. In the present structure, the corresponding angles are 12.5° for the imidazole ring on the mirror plane and 14.7° for the other independent imidazole ring. In each ring the bond vector deviates in the direction of the phosphorus atom. A movement of the Zn atom toward the P atom and an opening of the C–P–C bond angles both cause an increase in the amount of this deviation. Although the directional requirements for coordination bonds are not as stringent as those for covalent bonds, this deviation would likely be unfavorable. Thus the strain induced by the tridentate coordination of the ligand to Zn(II) appears to be distributed through the combination of a decrease in the C–P–C and N–Zn–N angles and an increase in the angles between the C–N–C bisectors and the N–Zn bonds.

The bond lengths and angles in the imidazole rings were compared with those of [bis(4,5-diisopropyl-1-methyl-2-imidazolyl) ketone]dibromozinc(II)[8] and tetrakis(imidazole)zinc(II) perchlorate[9] and did not differ significantly. The imidazole ring on the mirror plane is, of course, perfectly planar, and the nonmirror imidazole does not differ significantly from planarity (see Table II). The DMF molecule, as well, is essentially planar, and its bond lengths and angles do not differ greatly from previously published values.[13,14]

(13) Cobbledick, R. E.; Small, R. W. H. *Acta Crystallogr., Sect. B* **1973**, *B29*, 1659–1666.

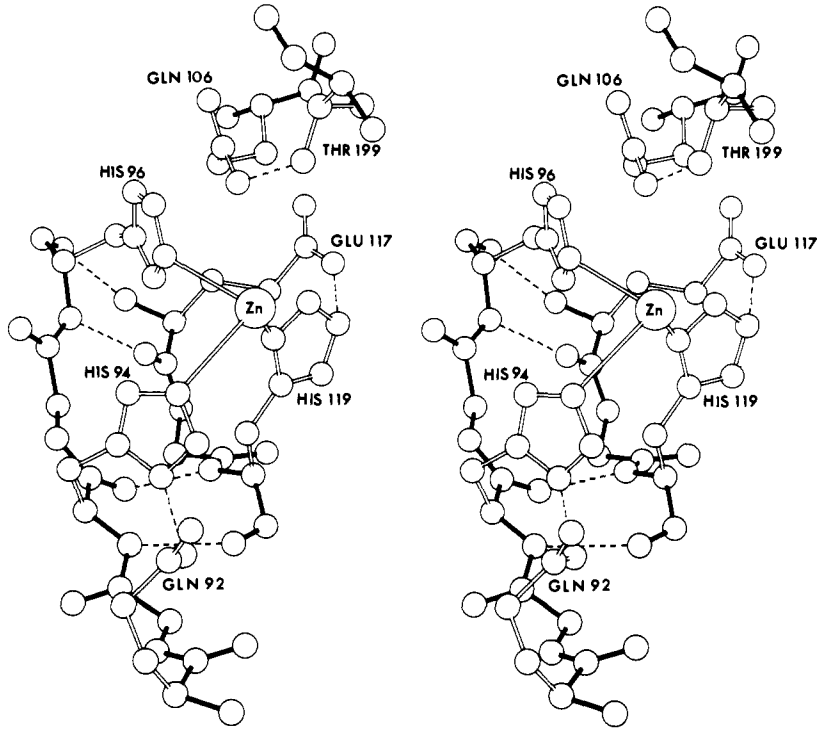


**Figure 4.** Stereoscopic view of the active site of HCAC. Filled bonds connect main chain atoms, and dashed lines indicate hydrogen bonds. Side chain atoms are included for only the labeled residues.

Table III. Bond Lengths (Å) Involving Hydrogen Atoms (esd's in Parentheses)

| | | | |
|---|---|---|---|
| N(1)-H(11) | 0.84 (4) | C(13)-H(133) | 1.03 (5) |
| N(3)-H(31) | 0.76 (2) | C(14)-H(141) | 0.94 (3) |
| C(4)-H(41) | 0.96 (4) | C(15)-H(151) | 0.94 (4) |
| C(5)-H(51) | 1.05 (6) | C(15)-H(152) | 1.04 (6) |
| C(5)-H(52) | 0.97 (4) | C(15)-H(153) | 0.96 (4) |
| C(5)-H(53) | 0.97 (5) | C(16)-H(161) | 0.84 (4) |
| C(6)-H(61) | 0.97 (4) | C(16)-H(162) | 1.00 (4) |
| C(7)-H(71) | 1.12 (4) | C(16)-H(163) | 0.99 (5) |
| C(7)-H(72) | 0.98 (4) | C(17)-H(171) | 0.92 (3) |
| C(7)-H(73) | 0.86 (4) | C(18)-H(181) | 1.07 (6) |
| C(11)-H(111) | 0.85 (5) | C(18)-H(182) | 0.87 (7) |
| C(12)-H(121) | 0.91 (5) | C(18)-H(183) | 0.90 (15) |
| C(12)-H(122) | 0.98 (4) | C(19)-H(191) | 0.99 (6) |
| C(12)-H(123) | 0.90 (5) | C(19)-H(192) | 1.13 (6) |
| C(13)-H(131) | 0.93 (5) | C(19)-H(193) | 1.02 (5) |
| C(13)-H(132) | 0.95 (5) | | |

Bond lengths involving H atoms (see Table III) are within the range expected for structures determined by X-ray methods. As shown in Figure 1, all **H** atoms in the methyl groups of the ligand are in the expected staggered conformation.

A staggered conformation is also observed for three of the four unique isopropyl groups, relative to the imidazole rings to which they are attached; the isopropyl groups attached to the imidazole ring on the mirror plane are constrained by this symmetry to adopt the staggered conformation. However, the isopropyl group consisting of C(11), C(12), and C(13) is twisted significantly from staggered conformation, as indicated by the difference between the torsion angles N(3)-C(9)-C(11)-C(12) (49.9°) and N(3)-C(9)-C(11)-C(13) (-85.5°). Figure 2 shows that C(12) is close to C(5) of the molecule translated 1 unit cell in the $x$ direction, and one observes relatively short interatomic distances from H(123) to C(5) (3.01 (5) Å) and H(53) (2.66 (7) Å) of the translated molecule. If the bond C(9)-C(11) is rotated to bring the isopropyl group into a staggered conformation, these distances become very close, i.e., 2.8 and 2.2 Å, respectively. Therefore, the deviation from a staggered conformation alleviates this potentially unfavorable interaction. One other point worth noting about the crystal packing is that the solvent DMF molecules are arranged in continuous channels parallel to [100].

There are two strong hydrogen bonds in the asymmetric unit, each involving one of the two unique imidazole N-H's. Cl(2) is 2.19 (4) Å from H(11) and 3.028 (3) Å from N(1), with an angle N(1)-H(11)-Cl(2) of 179 (3)°. O(1) of the DMF is 1.97 (2) Å from H(31) and 2.726 (3) Å from N(3), with an angle N(3)-H(31)-O(1) of 171 (2)°. The angle C(17)-O(1)-H(31) is 131.3 (7)°. Also, one may note in Table II that N(3) is very close (0.006 Å) to the plane of the DMF molecule.

A detailed comparison of the geometry of the present structure with the active site of carbonic anhydrase (see Figure 4 for the active site of HCAC) would be valuable but is not worthwhile at present, since the crystal structures of HCAB and HCAC are not refined.[15] In general, detailed examinations of protein structures which have not been extensively and carefully refined are dangerous, since coordinates can be in error by as much as 1 Å or more.[16] That such is the case in the carbonic anhydrase structures is indicated, for example, by the ligand N-Zn distances, which vary from 2.3 to 2.9 Å in HCAB and from 1.5 to 3.3 Å in HCAC, instead of the values of 2.0-2.1 Å that would be expected from small molecule structures.

The view of the HCAC active site in Figure 4 shows a number of serious stereochemical problems, in addition to the serious discrepancies in the Zn-N coordination distances, which are a result of not refining the structure. The hydrogen-bonding scheme proposed for the active site of HCAC,[2] which is almost identical with that proposed for HCAB,[17] is unreasonable for the following reasons. The plane of the amide of Gln-92 is almost perpendicular to the plane of the imidazole ring of His-94 (the dihedral angle between these two planes is 87°) and $O^{\epsilon 1}$ of Gln-92 is 1.7 Å from

(14) Ottersen, T.; Rosenqvist, E. *Acta Chem. Scand., Ser. B* **1977**, *B31*, 749-755.

(15) Coordinates for HCAB and HCAC used in this work come from the Brookhaven Protein Data Bank; see: Bernstein, F. C.; Koetzle, T. F.; Williams, G. J. B.; Meyer, E. F., Jr.; Brice, M. D.; Rodgers, J. R.; Kennard, O.; Shimanouchi, T.; Tasumi, M. *J. Mol. Biol.* **1977**, *112*, 535-542.

(16) Sielecki, A. R.; Hendrickson, W. A.; Broughton, C. G.; Delbaere, L. T. J.; Brayer, G. D., James, M. N. G. *J. Mol. Biol.* **1979**, *134*, 781-804.

(17) Notstrand, B.; Vaara, I.; Kannan, K. K. In "Isozymes I, Molecular Structure"; Markert, C. L., Ed.; Academic Press: New York, 1975; pp 575-599.

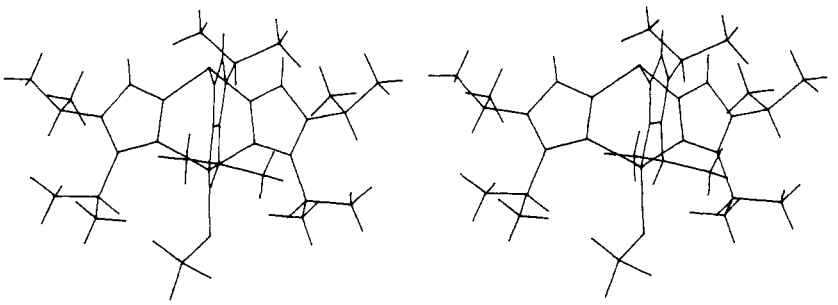

**Figure 5.** Stereoscopic view of the result of a model-building exercise in which Cl(1) was replaced by perchlorate.

Table IV. Selected Interatomic Distances from Model-Building Experiments with Halide Anions

| atoms | distances, Å | | |
|---|---|---|---|
| | X = Cl[a] | X = Br[b] | X = I[c] |
| C(7)-X | 3.671 (4) | 3.72 | 3.77 |
| C(15)-X | 3.734 (4) | 3.78 | 3.84 |
| C(16)-X | 3.790 (4) | 3.85 | 3.90 |
| H(72)-X | 2.82 (4) | 2.87 | 2.93 |
| H(152)-X | 2.90 (6) | 2.95 | 3.01 |
| H(162)-X | 2.92 (4) | 2.98 | 3.05 |

[a] Observed position of Cl(1). [b] Predicted position at $x = 0.567$, $y = 0.25$, and $z = 0.293$ in fractional coordinates. [c] Predicted position at $x = 0.568$, $y = 0.25$, and $z = 0.285$ in fractional coordinates.

the His-94 imidazole plane. As well, the plane of the carboxyl of Glu-117 is almost perpendicular to the plane of the imidazole of His-119 (the dihedral angle is 85°) and $O^{\epsilon 2}$ of Glu-117 is 2.8 Å from the His-119 imidazole plane. These features of the unrefined structure preclude the hydrogen-bonding scheme as proposed and make catalytic mechanisms for the hydrolysis of $HCO_3^-$ which invoke these hydrogen bonds equally tenuous.

Some general comparisons may be made between the carbonic anhydrase active site and the present structure. The general structural differences between the active-site analogue and the enzyme active site are mostly due to omissions in the analogue of components corresponding to other residues that are believed to contribute to the catalytic activity of the protein, such as Thr-199. Also, the ligand is structurally more rigid than the three histidine residues, which are more distantly connected; whether or not this is significant to catalytic activity is difficult to judge.

One chemical difference between the active-site analogue and carbonic anhydrase is in the order of relative strength of inhibition of catalysis by various anions. The strength of inhibition of HCAB and HCAC by anions follows the Hofmeister, or lyotropic, series; the order of inhibition is $ClO_4^- > I^- > Br^- > Cl^- > F^-$, which corresponds to the order of increasing negative hydration energies.[18] On the other hand, the order of inhibition for the analogue is $Cl^- > Br^- > I^- > F^- > ClO_4^-$.[3] In order to understand the reason for the differences in relative inhibitory activity, one must first understand the mechanism of anion inhibition. There is evidence that some inhibitory anions occupy a coordination site to Zn(II) in carbonic anhydrase,[19] either blocking the entry of $CO_2$ or displacing water or hydroxide. According to this scheme, anions which require more energy to desolvate will bind less tightly to Zn and thus will be less potent inhibitors. The difference in inhibition order for the analogue could be explained if perchlorate, iodide, and bromide were too large to fit without strain into the cavity occupied by Cl(1). In assessing this possibility, we performed model-building experiments in which Cl(1) was replaced by these three anions. The halide anions were placed on the Zn–Cl(1) vector at a distance of 2.36 Å from Zn for bromide, as observed in [bis(4,5-diisopropyl-1-methyl-2-imidazolyl) ketone]dibromozinc(II)[8] and a distance of 2.55 Å from Zn for iodide, as seen in [bis(pyridine)]diiodozinc(II).[20] Table IV gives the relevant interatomic distances for the observed structure with chloride and the model structures with bromide and iodide. While it is probably true that the fit becomes slightly tighter for the larger halides, the data in this table do not support a significant role for steric hindrance in the altered inhibition order for these anions. The situation for the perchlorate anion is somewhat more ambiguous. With an MMS-X interactive graphics system,[5] we performed a model-building experiment in which perchlorate was bound to Zn with the geometry observed in (perchlorotetraphenylporphinato)zinc(II).[21] With the ligand conformation observed in the crystal, it was not possible to find a conformation for perchlorate which did not have prohibitively close contacts. However, when each of the C(3)–C(6), C(10)–C(14), and C(10′)–C(14′) bonds was rotated by approximately 180°, the resulting model (see Figure 5) had no close contacts. The energy barrier for this rotation is likely to be quite high since in the course of the rotation of the lower isopropyl group, its methyl hydrogens will come into close contact with the hydrogen on the secondary C of the upper isopropyl group. However, the conformation depicted in Figure 5 is certainly not prohibited, since this is the conformation that is observed for the isopropyl groups of [bis(4,5-diisopropyl-1-methyl-2-imidazolyl) ketone]dibromozinc(II)[8]. It is difficult, then, to say whether or not steric effects lead to the discrepancy in inhibition of catalytic activity by perchlorate. One other factor may be relevant to the difference in order of relative inhibition of carbonic anhydrase and the active-site analogue. Since this order is related to the order of hydration energies of the anions, a difference in the hydration properties of these anions in the solvent mixture (80% ethanol–20% water) used in the kinetic experiments with the analogue[3] might contribute to a change in the order of relative inhibition.

**Note Added in Proof:** The crystal structures of HCAB (M. Ramanadham, personal communication) and HCAC (A. Jones, personal communication) are both being refined by least-squares methods. Intermediate results for each indicate a substantial improvement in the geometries of the Zn coordination and the hydrogen bonding.

**Acknowledgment.** We wish to thank R. S. Brown and J. Huguet for suggesting this study and for supplying the compound and L. Sawyer for valuable discussions. The Medical Research Council of Canada (MRCC) provided funds for this research. R.J.R. was supported during the course of this work by a studentship from the MRCC.

**Supplementary Material Available:** Table of anisotropic thermal parameters and a list of calculated and observed structure factor amplitudes (13 pages). Ordering information is given on any current masthead page.

(18) Maren, T. H.; Couto, E. O. *Arch. Biochem. Biophys.* **1979**, *196*, 501–510.
(19) Wyeth, P.; Prince, R. H. *Inorg. Perspect. Biol. Med.* **1977**, *1*, 37–71.
(20) LeQuerler, J. F.; Borel, M. M.; Leclaire, A. *Acta Crystallogr., Sect. B* **1977**, *B33*, 2299–2300.
(21) Spaulding, L. D.; Eller, P. G.; Bertrand, J. A.; Felton, R. H. *J. Am. Chem. Soc.* **1974**, *96*, 982–987.